

Multi-objective design optimization of a Quadrupole Resonator under uncertainties

Piotr Putek¹, Shahnam Gorgi Zadeh¹,
Ursula van Rienen^{1,2} Marc Wenkat^{3,4}

University of Rostock,

¹Institute of General Electrical Engineering,

²Department of Life, Light & Matter

³Universität Hamburg, Institute of Experimental Physics,

⁴Deutsches Elektronen-Synchrotron



Outline

Motivation

Reliable Simulations of QPR

- Parametrized model of QPR
- Stochastic Forward Problem
- Pseudo-spectral Approach

Result for MO robust shape optimization of QPR

- Formulation of MO robust optimization

Conclusions



Outline

Motivation

Reliable Simulations of QPR

Parametrized model of QPR

Stochastic Forward Problem

Pseudo-spectral Approach

Result for MO robust shape optimization of QPR

Formulation of MO robust optimization

Conclusions



Outline

Motivation

Reliable Simulations of QPR

- Parametrized model of QPR
- Stochastic Forward Problem
- Pseudo-spectral Approach

Result for MO robust shape optimization of QPR

- Formulation of MO robust optimization

Conclusions



Outline

Motivation

Reliable Simulations of QPR

- Parametrized model of QPR
- Stochastic Forward Problem
- Pseudo-spectral Approach

Result for MO robust shape optimization of QPR

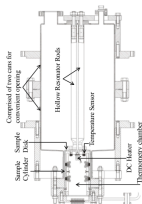
- Formulation of MO robust optimization

Conclusions

Sources of uncertainty in accelerator physics

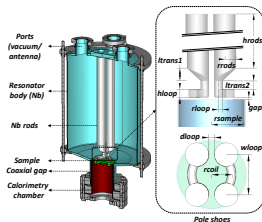
Reliable simulations of the superconducting radio-frequency cavity :

- input data & code uncertainties : measurement errors, error propagation
- modeling uncertainties : calibration and validation
- manufacturing uncertainties : ultrasonic bath, buffered chemical polishing, etc.
 - roughness of the superconducting surfaces
 - affect the material and geometrical parameters



QPR

Short characteristics of a device

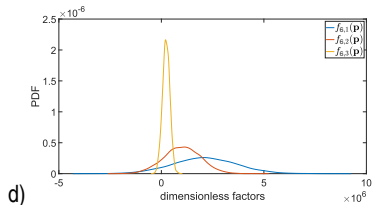
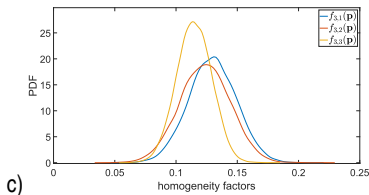


- special dedicated device used for the measurement of the surface resistance of superconducting samples at temperatures of 1.8 K to more than 20 K
- RF fields of up to 120 mT and operating frequencies of 433 MHz, 866 MHz and 1.3 GHz
- composed of a pillbox-like cavity containing four-vertically placed hollow rods
- quadrupole-like magnetic field is excited on the superconducting sample
- measurement data and expected losses on the sample allows for measuring the surface resistance of the sample with aid of calorimetric method

Consequences of Uncertainties

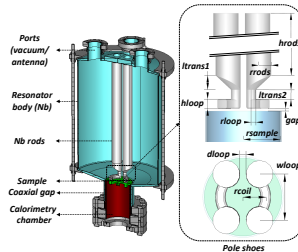
The measurement procedure is affected by various sources of uncertainties

- associated with the resolution of electronic equipment, geometrical deviations of a cavity design, and the accuracy of numerical simulations
- various figures of merit : a) operating frequencies – $f_0(\mathbf{p})$, b) focus factor – $f_1(\mathbf{p})$, c) homogeneity of the magnetic field distribution on the sample – $f_2(\mathbf{p})$, d) penetration of the magnetic field into the coaxial gap – $f_3(\mathbf{p})$



Parametrized model of QPR

A three-dimensional symmetric model (3D)



- as optimization of uncertain design parameters : $Q = 5$,
 $\mathbf{p} := (p_1, p_2, p_3, p_4, p_5)^T = (gap, rrods, hloop, rloop, wloop)^T$.
- geometrical imperfections related to the manufacturing of the QPR of order 50 – 100 [μm] are mimicked by the Gaussian distribution as follows

$$p_q(\xi) = \bar{p}_q(1 + \delta_q \cdot \xi_q), \quad q = 1, \dots, Q,$$

δ_q allows for controlling the magnitude of the perturbation such that $\sigma_q := \delta_q \cdot \bar{p}_q = 0.05$ [mm]



Stochastic Maxwell's Eigenproblem

Eigenpairs $(\mathbf{E}(\mathbf{p}), \lambda(\mathbf{p}))$:

$$\begin{aligned} -\nabla \times (\nu \nabla \times \mathbf{E}(\mathbf{x}, \mathbf{p})) + \lambda(\mathbf{p}) \epsilon \mathbf{E}(\mathbf{x}, \mathbf{p}) &= 0, && \text{in } D, \\ \mathbf{n} \times \mathbf{E}(\mathbf{x}, \mathbf{p}) &= 0, && \text{on } \partial D_P, \\ \mathbf{n} \times (\nu \nabla \times \mathbf{E}(\mathbf{x}, \mathbf{p})) &= 0, && \text{on } \partial D_N \end{aligned}$$

for $\mathbf{x} \in D \subset \mathbb{R}^3$, $\partial D = \partial D_P \cup \partial D_N$, $\mathbf{p} = (p_1, \dots, p_Q)^\top \in \Pi \subset \mathbb{R}^Q$

\mathbf{E} : phasor of electric field, $\lambda = \frac{\omega^2}{c^2}$: eigenfrequency, ω : angular frequency

c : speed of light, ν : magnetic reluctivity, ϵ : electric permittivity

Discretization : finite element method

(triangular mesh, piecewise linear functions)

UQ for Stochastic Forward Problem

Stochastic variables (Ω, Σ, μ) : $\mathbf{p}(\xi) = (p_1(\xi), \dots, p_Q(\xi))$, $\mathbf{p} : \Omega \rightarrow \Pi$,
independent, Gaussian, uniform, beta, etc.

Polynomial Chaos Expansion: a finite second moment of $f : [\lambda_0, \lambda_{\text{end}}]$:

$$f(\lambda, \mathbf{p}(\xi)) \doteq \sum_{i=0}^N v_i(\lambda) \phi_i(\mathbf{p}(\xi))$$

Based on calculations of a model at each quadrature points $\mathbf{p}^{(1)}, \dots, \mathbf{p}^{(K)} \in \Pi$:

$$\mathbb{E}[f(\lambda, \mathbf{p})] = v_0(\lambda), \quad \text{Var}[f(\lambda, \mathbf{p})] = \sum_{i=1}^N |v_i(\lambda)|^2$$

by using a multi-dimensional quadrature rule with weights $w^{(1)}, \dots, w^{(K)} \in \mathbb{R}$:

$$v_i(\lambda) := \langle f(\lambda, \mathbf{p}), \phi_i(\mathbf{p}) \rangle \doteq \sum_{k=1}^K w_k f(\lambda, \mathbf{p}^{(k)}) \phi_i(\mathbf{p}^{(k)})$$

Sensitivity analysis

Local sensitivity :

$$\left. \frac{\partial f}{\partial p_j} \right|_{p_j = \bar{p}_j} = \sum_{i=0}^N v_i \frac{\partial \phi_i}{\partial p_j} \frac{\partial \mathbf{p}}{\partial \xi_j}, \quad j = 1, \dots, Q.$$

Variance-based sensitivity :

$$S_j = \frac{V_j}{\text{Var}(f)} \quad \text{with} \quad V_j := \sum_{i \in I_j} |v_i|^2, \quad j = 1, \dots, Q,$$

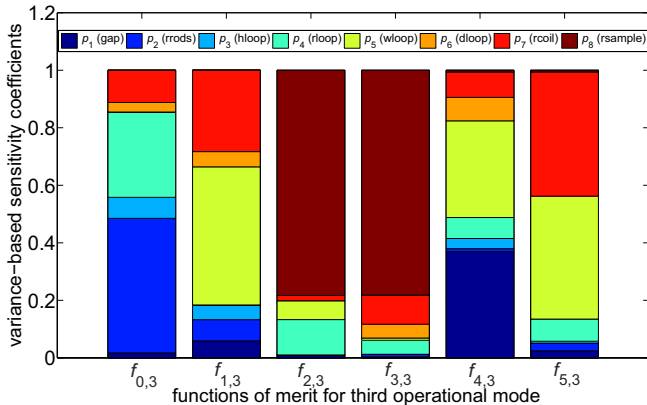
I_j : sets $I_j := \{i \in \mathbb{N} : \phi_i(\mathbf{p}) \text{ is not constant in } p_j\}$

$\text{Var}(f)$: the total variance

$0 \leq S_j \leq 1$: upper and lower bounds

UQ result for the end cell of QPR

Result for the variance based sensitivity analysis





Motivation

Reliable Simulations of QPR

Parametrized model of QPR

Stochastic Forward Problem

Pseudo-spectral Approach

Result for MO robust shape optimization of QPR

Formulation of MO robust optimization

Conclusions

Robust MO shape optimization

Random variables : $\xi = (\xi_1, \xi_2, \xi_3, \xi_4, \xi_5)$

Random dependent functionals :

$$[f_1(\mathbf{p}), f_2(\mathbf{p}), f_3(\mathbf{p})] = \left[\frac{1}{2U} \int_{\Omega_S} \|\mathbf{H}(\mathbf{p})\|^2 dx, \frac{\int_{\Omega_S} \|\mathbf{H}(\mathbf{p})\|^2 dx}{|\Omega_S| \max_{\mathbf{x} \in \Omega_S} (\|\mathbf{H}(\mathbf{p})\|^2)}, \frac{\int_{\Omega_S} \|\mathbf{H}(\mathbf{p})\|^2 dx}{\int_{\Omega_F} \|\mathbf{H}(\mathbf{p})\|^2 dx} \right]$$

Functionals for robust optimization :

$$\begin{aligned} & \inf_{\bar{\mathbf{p}} \in \mathbb{R}^Q} [\mathbb{E}(f_1), \mathbb{E}(f_2), \mathbb{E}(f_3)]^T \\ & \text{s.t. } \nabla \times (\nu \nabla \times \mathbf{E}(\mathbf{p}, \cdot)) - \lambda(\mathbf{p}, \cdot) \in \mathbf{E}(\mathbf{p}, \cdot) = 0, \\ & \rho_{L_q} \leq \bar{p}_q \leq \rho_{U_q}, \text{ for } q = 1, \dots, Q \end{aligned}$$

Approximation of probabilistic integrals :

Stroud-3 formula (10 nodes)



Parameters of stochastic simulation

Variations of geometrical parameters :

→ modeled by Gauss distribution

Random variations of parameters :

→ *gap*: $p_1 = \bar{p}_1(1 + \delta_1\xi_1)$

→ *rrod*: $p_2 = \bar{p}_2(1 + \delta_2\xi_2)$

→ *hloop*: $p_3 = \bar{p}_3(1 + \delta_2\xi_3)$

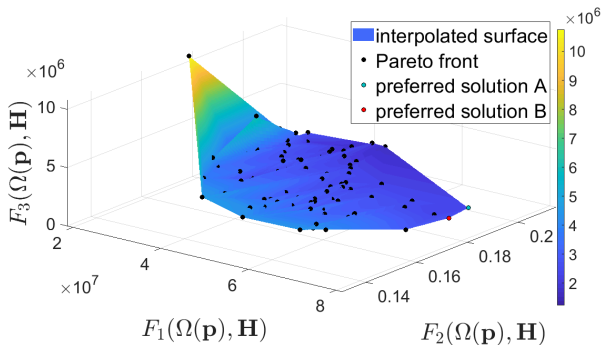
→ *rloop*: $p_4 = \bar{p}_4(1 + \delta_2\xi_4)$

→ *wloop*: $p_5 = \bar{p}_5(1 + \delta_2\xi_5)$

- independent normal random variables : $\xi_1, \xi_2, \xi_3, \xi_4, \xi_5$
- the magnitude of perturbation : $\sigma_q := \delta_q \cdot \bar{p}_q = 0.05$ [mm]

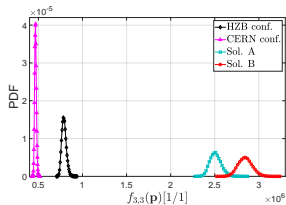
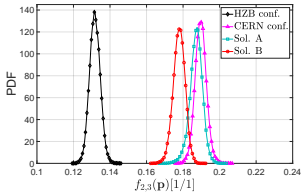
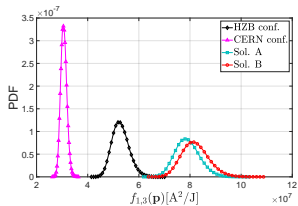
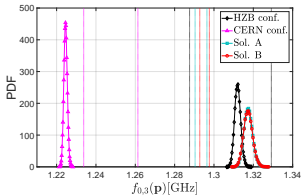
Robust MO Shape Optimization : Pareto front

VBS-MO shape optimization



Robust MO Shape Optimization : Pareto front

Probabilistic density functions



Robust MO Shape Optimization : shapes of QPR

VBS-MO shape optimization

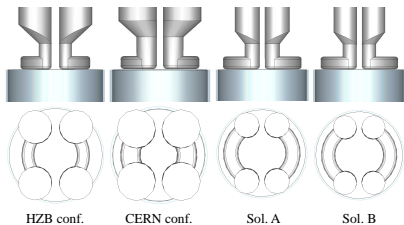


TABLE V. Results for the MO optimization – parameter domain ¹⁵

Name	$\Omega_{\text{HZB}}^*(\bar{\mathbf{p}})$	$\Omega_{\text{CERN}}^*(\bar{\mathbf{p}})$	$\Omega_{\text{A}}^*(\bar{\mathbf{p}})$	$\Omega_{\text{B}}^*(\bar{\mathbf{p}})$
p_1 (gap) [mm]	0.50	0.70	0.58	0.55
p_2 (rrods) [mm]	13.00	15.00	9.76	9.14
p_3 (hloop) [mm]	10.00	10.00	9.72	9.64
p_4 (rloop) [mm]	5.00	8.00	5.92	5.56
p_5 (wloop) [mm]	44.00	40.93	43.79	43.53
p_6 (dloop) [mm]	6.00	5.00	4.00	4.00
p_7 (recoil) [mm]	22.408	23.00	25.00	25.00
p_8 (rsample) [mm]	37.50	37.50	35.0	35.00

Robust MO Shape Optimization : summary

TABLE VI. Results of the MO optimization for the first mode – objective space ^a

Means/Configurations	$\Omega_{\text{HVB}}^*(\bar{\mathbf{p}})$	$\Omega_{\text{CERN}}^*(\bar{\mathbf{p}})$	[%]	$\Omega_{\text{A}}^*(\bar{\mathbf{p}})$	[%]	$\Omega_{\text{B}}^*(\bar{\mathbf{p}})$	[%]
$F_1(\Omega^*(\bar{\mathbf{p}}), \cdot)$ [M A ² /J]	50.07	32.15	-36.55	56.31	11.13	58.47	15.39
$F_2(\Omega^*(\bar{\mathbf{p}}), \cdot)$ [1/1]	0.155	0.218	41.15	0.227	48.84	0.216	39.70
$F_3(\Omega^*(\bar{\mathbf{p}}), \cdot)$ [M 1/1]	1.668	0.890	-46.64	3.941	136.3	4.421	165.1
$F_4(\Omega^*(\bar{\mathbf{p}}), \cdot)$ [1/1]	0.910	0.906	-0.43	0.901	-1.01	0.905	-0.62
$F_5(\Omega^*(\bar{\mathbf{p}}), \cdot)$ [mT/(MV/m)]	7.888	5.250	-32.93	4.824	-38.84	4.940	-37.38
$F_6(\Omega^*(\bar{\mathbf{p}}), \cdot)$ [GHz]	0.429	0.398	-7.21	0.439	2.21	0.439	2.23

^a The columns with percentage [%] indicate a ratio (increase +/decrease -) of optimized configurations to $\Omega_{\text{HVB}}^*(\bar{\mathbf{p}})$.

TABLE VIII. Results of the MO optimization for the third mode – objective space ^a

Means/Configurations	$\Omega_{\text{HVB}}^*(\bar{\mathbf{p}})$	$\Omega_{\text{CERN}}^*(\bar{\mathbf{p}})$	[%]	$\Omega_{\text{A}}^*(\bar{\mathbf{p}})$	[%]	$\Omega_{\text{B}}^*(\bar{\mathbf{p}})$	[%]
$F_1(\Omega^*(\bar{\mathbf{p}}), \cdot)$ [M A ² /J]	52.28	30.63	-42.05	78.98	49.43	82.04	55.21
$F_2(\Omega^*(\bar{\mathbf{p}}), \cdot)$ [1/1]	0.132	0.19	44.00	0.187	42.09	0.178	35.0
$F_3(\Omega^*(\bar{\mathbf{p}}), \cdot)$ [M 1/1]	0.791	0.467	-40.89	2.501	217.4	2.846	259.9
$F_4(\Omega^*(\bar{\mathbf{p}}), \cdot)$ [1/1]	0.914	0.917	0.3	0.907	-0.81	0.897	-1.94
$F_5(\Omega^*(\bar{\mathbf{p}}), \cdot)$ [mT/(MV/m)]	5.048	5.411	7.19	4.736	-6.18	4.685	-7.19
$F_6(\Omega^*(\bar{\mathbf{p}}), \cdot)$ [GHz]	1.312	1.225	-6.67	1.317	0.41	1.317	0.41

^a The columns with percentage [%] indicate a ratio (increase +/decrease -) of optimized configurations to $\Omega_{\text{HVB}}^*(\bar{\mathbf{p}})$.



Motivation

Reliable Simulations of QPR

Parametrized model of QPR

Stochastic Forward Problem

Pseudo-spectral Approach

Result for MO robust shape optimization of QPR

Formulation of MO robust optimization

Conclusions



Conclusions and further research

Conclusions :

- VBS robust MO shape optimization problem of QPR under uncertainties
- optimized configuration of QPR allows for increasing the focusing factor of the third mode by 50-57% and 158-168% compared to the HZB and CERN designs,
- better resolution of the surface resistance in different $freq_i$
- the dimensionless factor of $freq_3$ is more than twice bigger than for the HZB and CERN configuration
- it helps to decrease the measurement bias for the third mode in HZB and CERN designs

Further research directions :

- electro-stress-heat coupled problem of QPR & its optimization



Thank you for your attention